Bachelor Thesis

B.Sc. Physics of the Earth System:

Meteorology – Oceanography – Geophysics

Sea Level Variations in the New York Bay due to Various Parameters

Leon-Cornelius Mock

Matriculation Number: 1132992

December 13, 2021

First Reviewer: Prof. Dr. Arne Biastoch

Second Reviewer: Dr. Theo Gerkema

Christian-Albrecht University of Kiel

GEOMAR – Helmholtz Centre for Ocean Research Kiel

NIOZ – Royal Netherlands Institute for Sea Research

Abstract

Sea level rise is a topic of global importance and has amplified steadily in recent years. New York City and its adjacent bay have been particularly affected compared to the annual mean of the global rise of 3.4 mm since 1993. At the two sea level stations 'The Battery' and 'Sandy Hook', the annual increase over the same period even amounts to 3.9 mm and 5.2 mm. In addition to the long-term trend, however, there are fluctuations that mainly occur on smaller time scales within a year. Wind, air pressure and discharge of the Hudson River are influential parameters that are considered in this thesis. The winds from a southwesterly to northwesterly direction have by far the greatest influence lowering the sea level in New York Bay. In contrast, winds from northeast to southeast contribute to an increase in local sea levels. However, their influence is weaker, as the prevailing wind direction is west-northwest. Particularly strong influences can be captured during major storm events such as hurricanes or blizzards. While air pressure has a significant impact as well, this could not be shown for the Hudson River discharge.

Data Availability

The sea level data can be accessed via the website of the *Permanent Service for Mean Sea Level* (PSMSL) (https://www.psmsl.org/data/obtaining/stations/366.php and https://www.psmsl.org/data/obtaining/stations/12.php). Additionally, the ERA5 reanalysis with atmospheric variables by the European Center for Medium-Range Weather Forecast (ECMWF) (https://cds.climate.copernicus.eu/cdsapp#!/dataset/reanalysis-era5-single-levels?tab=overview) and discharge data of the Hudson River by the *Bundesanstalt für Gewässerkunde* (BFG) and the *Global Runoff Data Centre* (GRDC) (https://portal.grdc.bafg.de/applications/public.html?publicuser=PublicUser#dataDownload/Stations) was used.

Zusammenfassung

Meeresspiegelschwankungen in der New York Bay verursacht durch mehrere Parameter

Der Meeresspiegelanstieg ist ein Thema von globaler Bedeutung und hat sich in den vergangenen Jahren immer weiter verstärkt. New York City und die südlich angrenzende Bucht New York Bay sind im Vergleich zum globalen mittleren Anstieg von jährlich 3,4 mm seit 1993 besonders stark betroffen. An den zwei Meeresspiegelmessstationen „The Battery" und „Sandy Hook" beträgt der jährliche Anstieg im gleichen Zeitraum sogar 3,9 mm und 5,2 mm. Neben diesem Langzeittrend gibt es jedoch auch Schwankungen, die hauptsächlich auf kleineren Zeitskalen innerhalb eines Jahres geschehen. Wind, Luftdruck und Abfluss des Hudson River sind einflussreiche Parameter, die in dieser Arbeit betrachtet werden. Den größten Einfluss zeigen mit Abstand Winde aus einer südwestlichen bis nordwestlichen Richtung, die den Meeresspiegel in der Bucht senken. Dem entgegen gesetzt stehen Winde aus Nordost bis Südost, die an einer Erhöhung des lokalen Meeresspiegels beteiligt sind. Der Einfluss dieser ist jedoch niedriger, da die vorherrschende Windrichtung West-Nordwest ist. Besonders starke Einflüsse sind während großen Sturmevents wie Hurrikans oder Blizzards zu erkennen. Der Luftdruck konnte auch eine signifikante Auswirkung aufweisen, der Abfluss des Hudson River jedoch nicht.

Verfügbarkeit der Daten

Contents

List of Abbreviations

ECMWF	European Center for Medium-Range Weather Forecasts
NYB	New York Bay
PSMSL	Permanent Service for Mean Sea Level
RSL	Reconstructed Sea Level
SH	Sandy Hook (sea level station)
TB	The Battery (sea level station)

Main Variables

p	Air pressure on mean sea level	[hPa]
Q	River discharge	[m^3/s]
U	Absolute wind speed	[m/s]
u	Eastward wind component	[m/s]
v	Northward wind component	[m/s]
ρ	Air density	[kg/m^3]
φ	Wind direction	[deg]

Wind Directions

N	Northerly		*S*	Southerly
NE	Northeasterly		*SW*	Southwesterly
E	Easterly		*W*	Westerly
SE	Southeasterly		*NW*	Northwesterly

1 Introduction

Sea level variations, and sea level rise in particular, are of ever greater importance for humankind and are currently among the greatest threats to the entire environment. Around 45 per cent of the world's total population live in coastal areas (World Ocean Review 1, 2010). Of these, about 200 million people live less than five meters above sea level and are directly affected by the latest trend of sea level rise. By 2100 this number is expected to be at least twice as high. According to the 6th IPPC report from 2021, the global annual sea level rise has been around 1.7 mm from 1901 to 2018. However, recent satellite measurements by NASA (2021) even show annual ascension of 3.4 mm since 1993, corresponding to an average total rise of 100 mm in the last 29 years alone (Figure 1). Thermal expansion of the water is the dominant driver for the long-term trend, but there are also other causes (IPCC, 2021). Related factors are, e.g., ice loss from glaciers
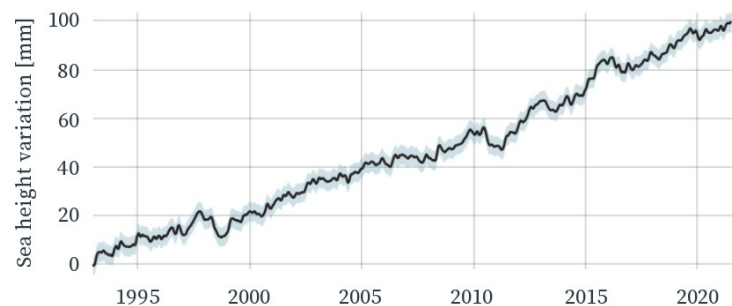
Figure 1: Global average sea level satellite data: 1993-present (reconstructed from NASA, 2021)

and ice sheets and changes in land-water storage. Factors on a more regional scale are land subsidence due to excessive extraction of groundwater which elevates the relative sea level, or the melting of permafrost and the subsequent release of trapped methane which in turn causes further heating of the atmosphere.

It is important to be aware that there is not only *long-term* sea level rise induced by climate change. Equally, there are fluctuations on decadal and *short-term* interannual timescales, where river discharge and atmospheric parameters such as wind, air pressure and precipitation are dominant drivers. These factors should generally not be underestimated since they often pose an even greater danger as the long-term trend due to unpreparedness. For this reason, already one of those parameters alone can cause enormous damage, even inland and far from the
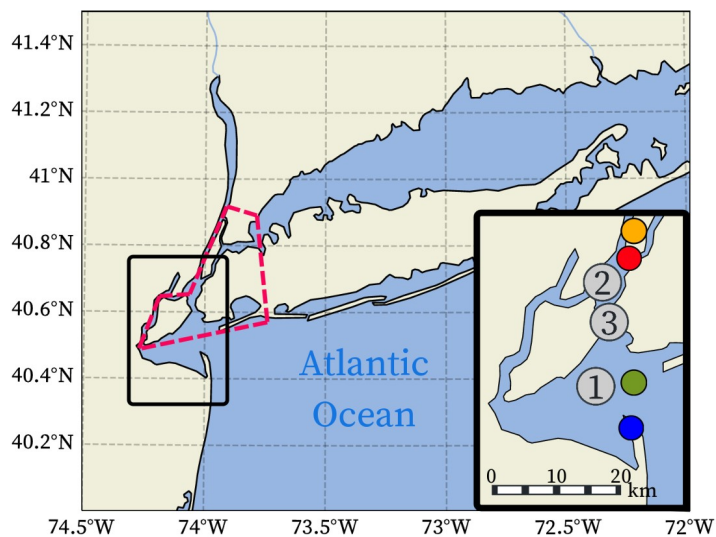
coast. As a recent example, in the spring of this year, heavy rainfall hit the border region of Belgium, Luxembourg, the Netherlands and Germany. In the German state of Rhineland-Palatinate, the small river Ahr quickly overflowed its banks, claiming 134 fatalities in this region (ADD-RLP, 2021). To this day, the infrastructure is gravely damaged, and the economic loss in Germany is currently estimated at up to 30 billion US dollars (BMI, 2021), which is a record sum for Europe (Aon, 2021). If even more parameters have an influence, the radius of destruction can be of a much bigger dimension, especially in vulnerable coastal regions. That is the case with sudden floods due to tropical storms associated with extreme winds such as Hurricane Katrina, which hit large parts of the southeastern United States, Cuba, and the Bahamas in 2005, causing an economic damage of 108 billion US dollars (National Weather Service, 2016).

New York City and its bay, which is the location of interest for this thesis, was spared from damages during Hurricane Katrina. However, the region was hit by other hurricanes with severe effects, e.g., Sandy in 2012 or Ida in 2021. Sandy was the most destructive hurricane on record after Katrina and caused a storm-tide of 3.48 m above mean tide level (Blake et al., 2013). Heavy floodings also occurred several other times, e.g. in 1938, 1960 and 1985 (Kemp and Horton, 2013), even though New York City is situated comparatively far north on the North American continent to be badly affected by hurricanes, as can be deduced from records by the National Hurricane Center (2021a). Tropical storms usually weaken when they pass landmass, or they do not even reach the continent and move directly eastward across the Atlantic while weakening there over time. For this reason, New York City does not deal with major hurricane strikes quite as frequently and intensively as, e.g., the southeastern United States. Not only are floods caused by tropical storms, but also by winter cyclones in particular, with 12 storms a year on average (Colle et al., 2010). They come predominantly from the northeast, which is why they are commonly referred to as the 'Nor'easters'. Recent popular events

are a 1.75 m storm surge in 1992 (Colle et al., 2008) or Blizzard Nemo in 2013. It is expected that in the future the 'Nor'easters' will even intensify in years of El Niño events (Colle et al., 2010). Apart from the hurricanes and 'Nor'easters', there are other storms throughout the year, most of which come from the northwest. Thus, there is a constant hazard to New York City and its inhabitants all year round. The area is densely populated with roughly 12 million people living in immediate vicinity of the New York Bay and its surrounding counties (U.S. Census Bureau, 2019).

The New York Bay (NYB) is located in the states of New Jersey and New York in the northeastern United States and has access to the Atlantic Ocean. In the following of this thesis, two sea level stations around NYB are investigated (see Figure 2, and Section 2.1). As a tidal estuary, the Hudson River mouth lies within the urban area of New York City and opens up into the northern part of the NYB, the Upper New York Bay. Analogously, the southern part is known as Lower New York Bay. Both water bodies are connected by 'The Narrows'. The Hudson River

Figure 2: New York Bay south of New York City (red dashed line) with Lower New York Bay (1), mouth of Hudson River in Upper New York Bay (2) and the connecting 'Narrows' (3); Location of datasets: Sealevel at 'Sandy Hook' (blue) and 'The Battery' (red), and ERA5 reanalysis data (green & orange)

and the NYB continue to drain into the Atlantic Ocean through the submarine Hudson Canyon. Tidal estuaries are generally fragile systems that are sensitive to flooding (Zhong et al., 2013). Different volumes of river discharge have an influence on how far the sea, here the New York Bay, flows into the river and pushes inland.

The aforementioned Hurricanes Sandy and Katrina sparked discussion in New York City about building storm surge barriers (e.g., Royte, 2019, and Hill, 2008). Recently, construction for breakwaters and development of seawalls has started in New York City (CEG, 2021). Before Hurricane Katrina, the city of New Orleans, e.g., had levees and flood walls, but they broke and could not withstand the enormous water masses. It is precisely for this reason that proper coastal protection systems are of great importance. Building them should be considered after careful examination of which areas are affected and what the main drivers are. The Netherlands is an example of how this can be achieved. A flood disaster, the 'Zuiderzeevloed' in 1916, provoked a public call for protection from the North Sea. Even as early as in the 1920s, dams, reclamation areas and water pumping systems were constructed around the Zuiderzee, today's IJsselmeer. The 'Deltawerken' were built in the province of Zeeland after the 1953 North Sea flood. Together with the 'Zuiderzeewerken', they are among the seven wonders of the modern world (ASCE, 1995). The numerous dams made land reclamation and flood protection possible on a large scale. In fact, around 20% of the land area of the Netherlands was reclaimed, including the entire province of Flevoland, and even a total of 26% of the country is actually below sea level. It is estimated that around 59% of the Dutch land area are at great risk from floods (Tijburg, 2021).

Regardless of whether or not further storm surge barriers are ultimately built in the New York Bay, it is important to keep track of any fluctuations in sea level. It is expected that the relative sea level in the NYB will further rise which will even aggravate floodings due to hurricanes (Kemp and Horton, 2013) or other storms. Therefore, this thesis mainly investigates the following questions:

1) What is the general development of the regional sea level in the New York Bay over the period from 1981 to 2020?
2) What properties do wind, air pressure and river discharge of the Hudson River have there and what are their influences on the sea level signal?
3) Are there any other dominant parameters?

2 Data and Methods

The requirement for the datasets was to offer significant time spans and, of course, to be as precise and spatially covering as possible for the New York Bay. In order to obtain reliable values in a climatological sense, at least 30 years of data should be considered. Two suitable sea level stations with a long record were found and linked to atmospheric reanalysis data. Lastly, discharge data from the Hudson River was applied.

2.1 Sea Level Data

The Permanent Service for Mean Sea Level (PSMSL) provides global data records from tide gauges for the sea level. At station 366 'Sandy Hook' (40°28'00" N, 74°00'30" W; Figure 2, blue), data is available in monthly means starting in 1932. The station is situated in the north of the Sandy Hook peninsula which is surrounded by Sandy Hook Bay in the west, Lower New York Bay in the north and the Atlantic Ocean to the east. Across NYB, at the southern tip of Manhattan and the mouth of the Hudson River, station 12 'The Battery' (40°42' N, 74°01' W; Figure 2, red) is located. Data from this station is available since 1856 with a gap from 1879 to 1892. In order to agree with the reanalysis data, both sea level datasets were effectively only used from 1981 onwards. The so-called 'Revised Local Reference' diagrams confirm that there were no changes in the position of the measuring devices or no other influences that may have affected the sea level baseline during the operation of the stations (PSMSL, 2021a and 2021b). Therefore, the data sets are qualified for research use (Holgate et al., 2013). Further stations in this area are not suitable for this time period. But still, the selected stations cover both of the main parts of the NYB.

2.2 ERA5-reanalysis for Atmospheric Data

Due to restricted access to observational atmospheric data for periods with a similar time span as that of the sea-level records, the ERA5-reanalysis was used. ERA5 is a climate reanalysis by the European Center for Medium-Range Weather Forecast (ECMWF) from 1950 to present. However, only the data for the entire years 1981 to 2020 was used since an earlier period of ERA5 is only available as a preliminary version. The hourly reanalysis data originates from satellite measurements, supplemented by data from, e.g., radar gauges and aircraft, and is combined with numeric models (Hersbach et al., 2020). ERA5's spatial resolution of 0.25° for both longitude and latitude allowed to find separate data for both sea level stations. A data point right off the entrance of NYB (40°30'N, 74°00'W; Figure 2, green) was used for 'Sandy Hook' and another one in Manhattan (40°45'N, 74°00'W; Figure 2, orange) for 'The Battery'. The exact distance to the corresponding sea level stations is 3.7 km and 5.6 km, respectively.

Wind data was extracted at the height of 10 meters in three-hour intervals. In order to properly utilise the wind data, calculations with additional variables were necessary (see Sections 2.2.1 and 2.2.2). That included air pressure, air temperature and dew point temperature on mean sea level. The air pressure values were also considered separately and could be used without preceding calculations.

2.2.1 Wind

ERA5 provides the u- and v-component of the wind, the eastward and northward values, respectively. They can be used to calculate absolute wind speed U and direction φ (Figure 3).

$$U = \left| \vec{U} \right| = \left\| \begin{pmatrix} u \\ v \end{pmatrix} \right\| = \sqrt{(u^2 + v^2)} \tag{1}$$

$$\varphi = mod \left(180^o + \frac{180^o}{\pi} \arctan 2 \left(u, v \right), \, 360^o \right) \tag{2}$$

Pythagoras' theorem (1) yields U, whereas equation (2) results in φ in degrees for the 'North-Clockwise'-convention. This means, e.g., 0° correspond to a northerly or southward wind and 90° to an easterly or westward wind, as can be seen in Figure 3. To avoid confusion, it should be noted that the suffix '-erly' indicates the direction *from* which the wind is coming, while '-ward' denotes the direction *in* which the wind is blowing.
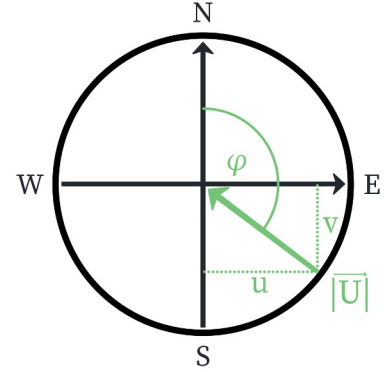
Figure 3: Visualisation of the wind variables

In order to investigate the influence of wind on the sea level, the wind energy for each sector of the eight cardinal and ordinal directions was used. As an alternative approach, Gerkema and Duran-Matute (2017) mention the use of wind stress but argue that the drag coefficient would then have to be determined for all kinds of wind strengths. They refer, e.g., to Guan and Xie (2004), where the drag coefficient initially depends linearly on the wind speed. In combination with the factor U^2 that indicates a cubic power of U in stress; so does the wind energy without a complex determination of drag coefficients. While assuming the sea surface to be flat, the kinetic wind energy E_n passing an area A was calculated in joule [J] with the following equation (3) from Gerkema and Duran-Matute (2017):

$$E_n = \frac{1}{2} \, m \, U_n^2 = \frac{1}{2} \, \rho \, V \, U_n^2 = \frac{1}{2} \, \rho \, A \, \Delta t \, U_n^3 \tag{3}$$

where $n = N, NE, \ldots, NW$ acts as the wind sectors starting with northerly (N) and continuing clockwise to northwesterly (NW). The exact calculation of the air density ρ is explained in section *2.2.2*. A is taken as $1\,m^2$ and Δt as an hourly time interval in seconds. The mass m of an air volume $V = 1\,m^3$ was not further needed.

2.2.2 Air Density

The spatial resolution of the density ρ grid does not appear to be as high as the rest of ERA5, or there are not enough values available for this area. Only one data

point with missing values was found. Therefore the density had to be calculated separately from air pressure, air temperature T and dew point temperature D. An assumption of a constant value would be sufficient as ρ is not subject to strong fluctuations with roughly 15 % spread. However, in the course of estimating an accurate mean value for the area, the entire computation of ρ does not involve any significant additional effort. The calculation of one value and that of all is almost equal in time. Thus, all values can be calculated simultaneously. Considering moist air, the air density can be described as:

$$\rho = \frac{p_d}{R_d T} + \frac{p_v}{R_v T} \tag{4}$$

where $R_d = 287.05\,\text{J/(kg K)}$ and $R_v = 461.50\,\text{J/(kg K)}$ are the specific gas constants and p_d and p_v the partial pressures of dry air and water vapour. The sum of the partial pressures is the total air pressure p, meaning p_d results from the subtraction of p_v, which is to be calculated, from p, which is provided by ERA5.

$$p_v = \frac{e_{SO}}{\left(c_0 + D\left(c_1 + D\left(c_2 + D\left(c_3 + D\left(c_4 + D\left(c_5 + D\left(c_6 + D\left(c_7 + D\left(c_8 + D(c_9)\right)\right)\right)\right)\right)\right)\right)\right)\right)^8} \tag{5}$$

Hermann Wobus, a former mathematician at the Navy Weather Research Facility in Norfolk, Virginia (USA), developed the polynomial formula (5) to describe water vapour pressure in hectopascal [hPa]. However, when returning to equation (4), the pressures p_d and p_v should be used in pascal [Pa]. Wobus's approximation is stated to be applicable for temperatures between -50 °C and 100 °C (Schlatter and Baker, 1991). Contrary to T in (4), the dew point temperature D is used in degrees Celsius [°C]. e_{SO} is the saturation vapour pressure over liquid water at 0°C. The constants $c_0, c_1, ..., c_9$ are displayed in Table 1. They were empirically determined by Wobus to fit the Smithsonian meteorological tables (Schlatter

CONSTANT	VALUE
e_{SO} [hPa]	6.1078
c_0 [°C^{-1}]	0.99999683
c_1 [°C^{-1}]	$-0.90826951 \cdot 10^{-2}$
c_2 [°C^{-1}]	$0.78736169 \cdot 10^{-4}$
c_3 [°C^{-1}]	$-0.61117958 \cdot 10^{-6}$
c_4 [°C^{-1}]	$0.43884187 \cdot 10^{-8}$
c_5 [°C^{-1}]	$-0.29883885 \cdot 10^{-10}$
c_6 [°C^{-1}]	$0.21874425 \cdot 10^{-12}$
c_7 [°C^{-1}]	$-0.17892321 \cdot 10^{-14}$
c_8 [°C^{-1}]	$0.11112018 \cdot 10^{-16}$
c_9 [°C^{-1}]	$-0.30994571 \cdot 10^{-19}$

Table 1: Wobus' constants

and Baker, 1991) which describe the state of the atmosphere through observations and give values for p_v at specified temperature levels (Bull, 1952). Although this formula dates back at least 40 years and is based on values from 1951, it seems to be precise and is still used regularly for similar applications, e.g., in Brito et al. (2014) or Firtina-Ertis et al. (2020).

The resulting values of this calculation range from $1.132\,kg/m^3$ to $1.425\,kg/m^3$ for the data point which was assigned to 'Sandy Hook' and from $1.120\,kg/m^3$ to $1.447kg/m^3$ for 'The Battery'. Also, the mean values are close to each other with $1.2358\,kg/m^3$ and $1.2361kg/m^3$, respectively. Therefore, the values used for both stations are similar but on some occasions there are larger deviations from the means.

2.3 River Discharge

As the last parameter, discharge data Q of the Hudson River was accessed from the Global Runoff Data Centre (GRDC). Daily mean data is available from 1946 onwards, but there is a gap in the period under review from October 1997 to September 2000 and December 2020 is missing. A proper analysis is problematic, since the only data point which can be considered to some extent is located around 240 km upstream in Green Island, New York. Because of this distance, corrections have to be made. It is to be expected that over the distance from the measuring station to 'The Battery' there will not only be a change in the water volume but also a time shift. However, in Ralston et. al (2008) (referring to Lerczak et. al, 2006) the data from Green Island was only multiplied by a factor of 1.6. With this simplification, good results were achieved there.

2.4 Correlations and Sea Level Reconstruction

Single and multivariate correlations were used as a measure of the influence of the individual parameters on sea level. As in Gerkema and Duran-Matute (2017), a linear dependence of the sea level on wind energy or air pressure was

preliminarily assumed. Later, during a graphical analysis of the correlations, this remained plausible. Pearson's coefficient, which is the ratio of the two variables' covariance and the product of their standard deviations (KSU, 2021), was used as the coefficient for the individual correlations. In order to assess which correlation coefficients are significant, the degrees of freedom of the data were determined. If there is no statistical time dependency, the degrees of freedom are *N-2*, with *N = 40 years · 12 months = 480* as the total length of the data set. This statistical time dependency can be identified with the help of autocorrelations. To do that, the sea level data was correlated with itself and gradually shifted by each time step ('lag'). Following this, the original number of degrees of freedom was divided by the first lag, which
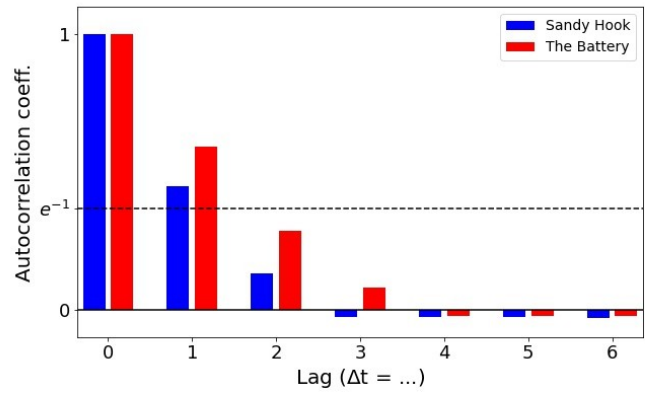
Figure 4: Coefficients for the autocorrelation for both sea level stations and with lags in time steps

yielded a correlation coefficient of less than the reciprocal of Euler's number (e^{-1}). The autocorrelations of both sea level datasets resulted in a lag quotient of 2 (see Figure 4). Consequently, the effective degrees of freedom are *(N-2)/2 = 239*. According to Stephenson and Kolli (1997), already correlations of ±0.1278 and ±0.1675 are 95 % and 99 % significant for this number of degrees of freedom.

With the help of multivariate regression, the sea level was reconstructed using the individual correlation coefficients k_i from a multiple correlation and then compared to the original measurement values.

$$RSL = b + \sum_{i=1}^{j} k_i x_i \qquad (6)$$

Equation (6) describes the reconstructed sea level (RSL), with *i = 1, 2, 3,..., j* and *j* as the total number of inspected variables, x_i as the values for each variable, and the intercept *b* with the vertical axis.

3   Results

This section presents an overview of the general conditions, trends, and the outcomes after using the methods discussed in section 2. Each variable is assigned to its own sub-chapter and is first observed individually and finally interlinked altogether.

3.1 General Overview of the Properties and Trends of all the Parameters
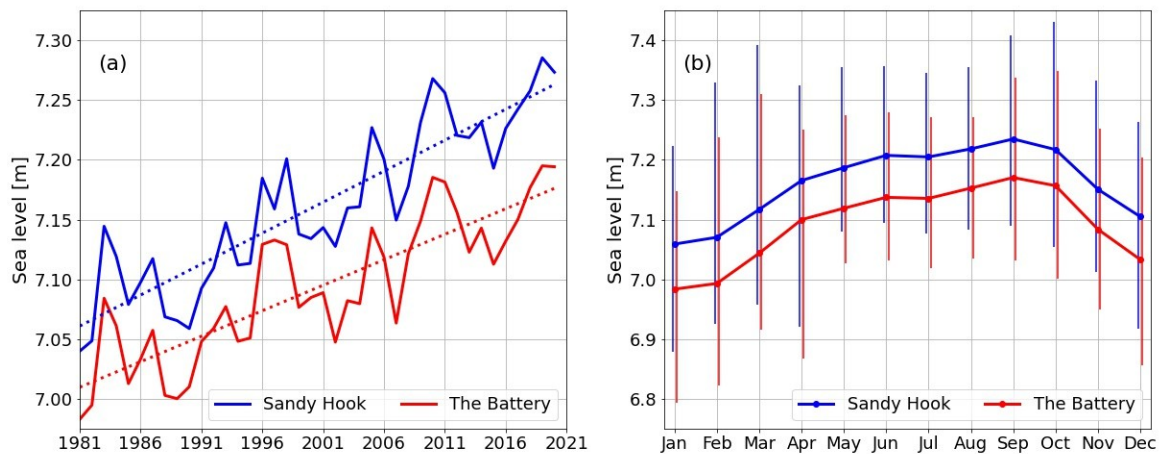
3.1.1 Sea Level

In 1932, when the station at 'Sandy Hook' was established, and until 1950, sea level at both inspected stations was at the same height. Since then, the sea levels at both stations have risen differently (Figure 5). The annual mean sea level rise has been 4.1 mm at 'Sandy Hook' and 3.1 mm for 'The Battery'. When considering the time period from 1993 to 2021 as in Figure 1 for the global picture, the annual increase is even 5.2 mm and 3.9 mm. Both values are above the global mean with 51.8 % and 14.7 %, respectively. This suggests that the sea level rise is particularly strong in the New York Bay and that sea levels can vary widely, even
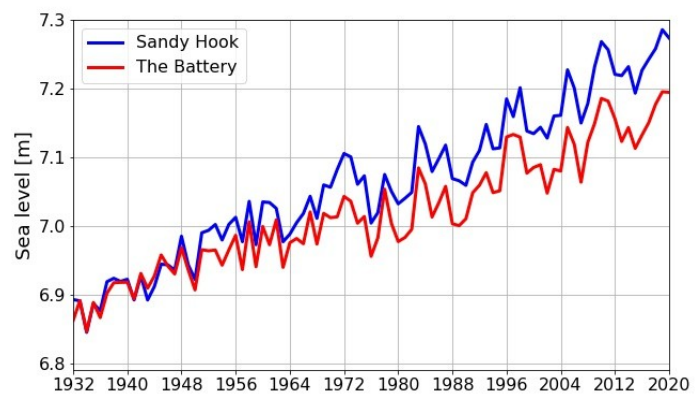
Figure 5: Annual mean sea level data at the two inspected stations 'Sandy Hook' and 'The Battery'

within a small area. The observation over the longer period since 1932 is necessary, as the discrepancy is initially not apparent when only looking at the actual inspected period from 1981 to 2020. For both the annual mean sea level (Fig. 6a) and the seasonal cycle (Fig. 6b), the sea level records follow the same course and therefore seem to be subject to the same forces. At this point of time, the long-term trend has not yet been deducted for the sake of illustration, but this

Figure 6: Long-term trend and seasonal cycle of sea level in NYB – In **(a)**, the monthly data is displayed in annual means. Dotted lines represent the least squares fit. **(b)** shows mean sea level values for each month of the year as an average of the respective months from 1981 to 2020. The vertical lines represent the range from the maximum to minimum values.

is the case for the later calculation of the correlations which are for the monthly data anyway. During the year, the sea level increases almost monotonically from January to September, but on average, there is a minimal drop from June to July. The greatest rising slopes are to be found from February to April and the strongest decline from October to December. Maximum and minimum values span the largest difference from September or October to April with up to ±0.22 m in the monthly mean.
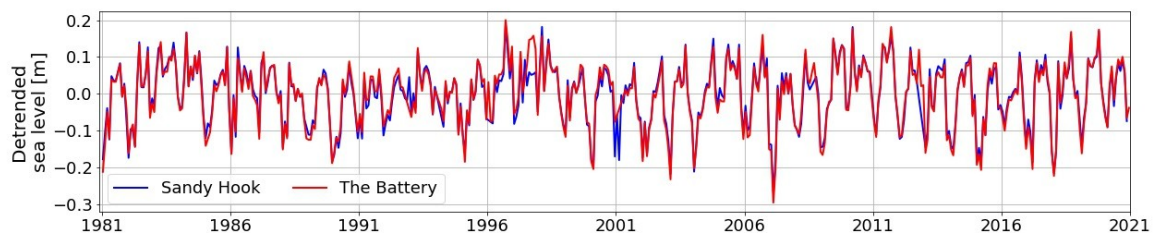
Figure 7: Detrended monthly mean sea level for sea level stations 'Sandy Hook' and 'The Battery'

If a linear fit similar to the one in Figure 6a is deducted from the monthly sea level data, the sea level is detrended (Figure 7). Here, the graphs of the two stations follow an almost identical course as well, so that both curves overlap on many occasions. The similarity of the sea level courses is confirmed by their correlation coefficient of 0.983. The individual years can also be identified through the seasonal cycle as shown in Figure 6b with an increase towards summer and a decrease towards winter. On average, the sea level fluctuates around 0.1 to 0.2 m.

3.1.2 Wind

To simplify the notation, the ERA5 data points that are assigned to the stations 'Sandy Hook' (SH) and 'The Battery' (TB) are referred to as such in the following. Figure 8 depicts the resolution of the ERA5 grid and the mean state for the wind. The New York Bay is resolved by roughly four grid points, but strictly speaking, only the two points used are directly adjacent to the NYB, and to both sea level stations.
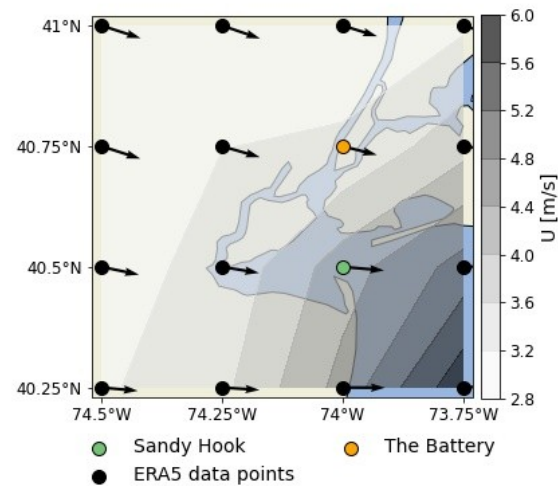
Figure 8: Distribution of mean wind speed and wind direction in the NYB area based on the ERA5-reanalysis over the period from 1981 to 2020

As can be seen in Figures 8 and 9, the dominant wind direction is westerly or northwesterly. Likewise, the majority of the winds with higher wind speeds come from these same sectors. With around 8 % of the total share each, easterly and southeasterly winds are the least represented. Given the location in the westerly
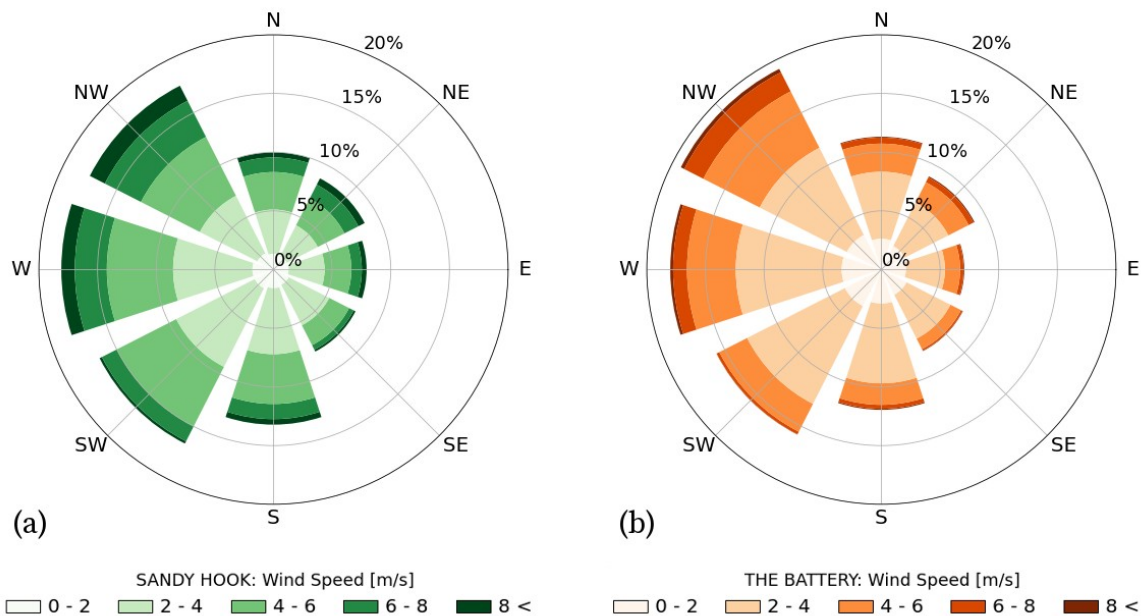
Figure 9: Wind roses with percentage distribution (1981-2020) of wind directions (N ≘ northerly) for two separate ERA5 data points closest to the sea-level stations at 'Sandy Hook' **(a)** and 'The Battery' **(b)**. The wind speeds are classified in 5 groups and the directions in 8 sectors.

wind zone, this is not surprising. Since both reanalysis data points are close to each other, it is reasonable that the distribution of wind direction sectors is similar for both locations. However, there are differences in wind speeds and strengths. By dividing the wind speeds into classes, it becomes clear that the winds at SH are faster than at TB. This is also proven by the average speeds of 4.21 m/s and 3.23 m/s, respectively. At 'Sandy Hook', winds of the highest constructed class occur at least five times more often than at 'The Battery'. In addition to that, weak winds of the lower two classes occur to 73 % at TB, instead of only 51 % at SH. As 'The Battery' is located inland and in the inner-city of New York City, there is a higher effect of friction reducing the wind there than at 'Sandy Hook', which is more exposed to the open sea. Already Figure 8 with the general mean values shows that the wind speed increases with increasing distance from to the interior.
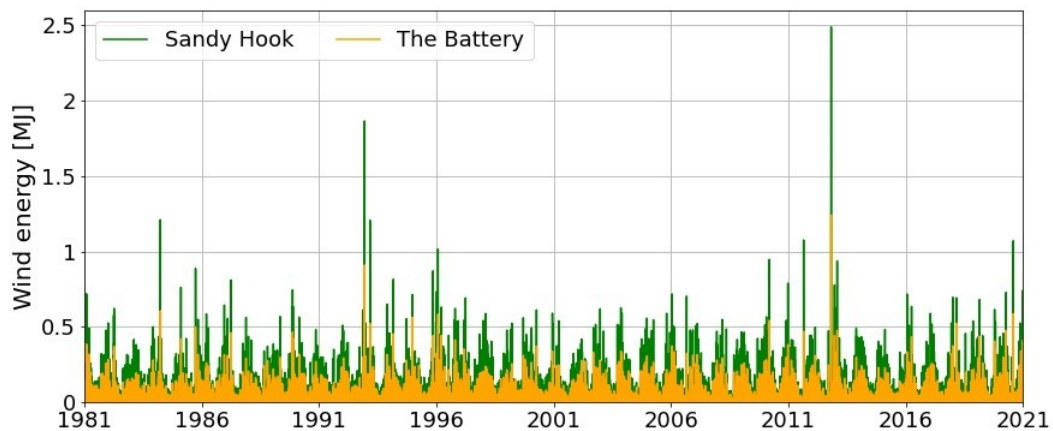
Figure 10: Daily mean wind energy in $\Delta t = 1h$ from 1981 to 2020 based on the ERA5-reanalysis

In contrast to sea level, there is no discernible long-term trend for wind energy (Figure 10). Over the entire period from 1981 to 2020 there are repeatedly similar fluctuations. What is striking is that there are large wind energies in the winters of 1992/1993 and 2012/2013 with up to 1.85 MJ and even 2.5 MJ. They correspond to a 'Nor'easter' on December 11, 1992 and Hurricane Sandy with its local maximum on October 30, 2012. Due to lower wind speeds, the total wind energy at 'The Battery' is lower as well. TB's values are exceeded by SH, which on average are twice as high for the most of the year. Since there is a difference in the

behaviour of the sea level (see Fig. 6b) between the summer and winter months, it was reasonable to check a seasonality for the wind as well (Figure 11). The total wind energy of all sectors combined is highest from November to March for both SH and TB with around 0.42 MJ and 0.19 MJ, respectively. That means that the sum of the
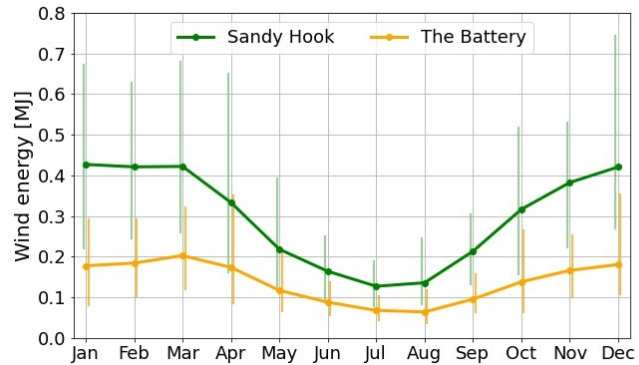
Figure 11: Seasonal cycle of the wind energy based on the ERA5-reanalysis - Monthly mean total wind energy in Δt=1h for each month of the year as an average of the respective months from 1981 to 2020. The vertical lines represent the range from the maximum to minimum values.

wind energy is mainly not influenced by the tropical storms during the Atlantic hurricane season from June to November (National Hurricane Center, 2021b) but by the winter storms which occur at a higher frequency. In accordance with the seasonal cycles of sea level and wind, and supplementary to the all-year examination, the summer half-year (from April to September) and winter half-year (from October to March) were both observed individually. The sectorial distribution of the wind speeds is also reflected in wind energy (Figure 12). In the individual sectors, too, energy is twice as high at SH than at TB. Northeasterly energy and thus the 'Nor'easters' are slightly below the averages of 37 kJ and 17 kJ. In general, most of the wind energy comes from the west and northwest. When
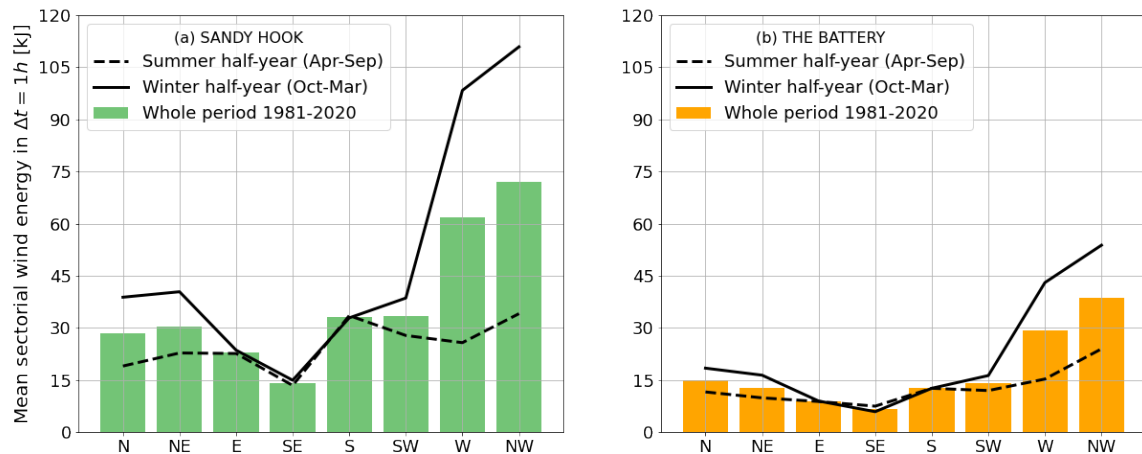

Figure 12: Sectorial wind energy (N ≙ northerly) in temporal means of one hour for two separate ERA5 data points closest to the sea-level stations at Sandy Hook **(a)** and The Battery **(b)**. Data for the whole period, and the summer half-year and winter half-year are displayed separately.

looking at the half-year analysis, it is noticeable that wind energy is higher in winter than in summer, as soon as a northerly or westerly component is involved. Between the half-years, there is no clear difference noticeable for the easterly to southerly winds.

3.1.3 Air Pressure

Since the sea level data is only available in monthly averages, the air pressure is also considered in these time intervals. However, this causes exceptional deflections to be lost. The monthly means can be seen in Figure 13a. The pressure is almost the same for both data points and changes around the mean value of 1016.7 hPa with approximately ±7 hPa. Actual minimum and maximum values are of course not within this range. Over the entire period, the highest air pressure
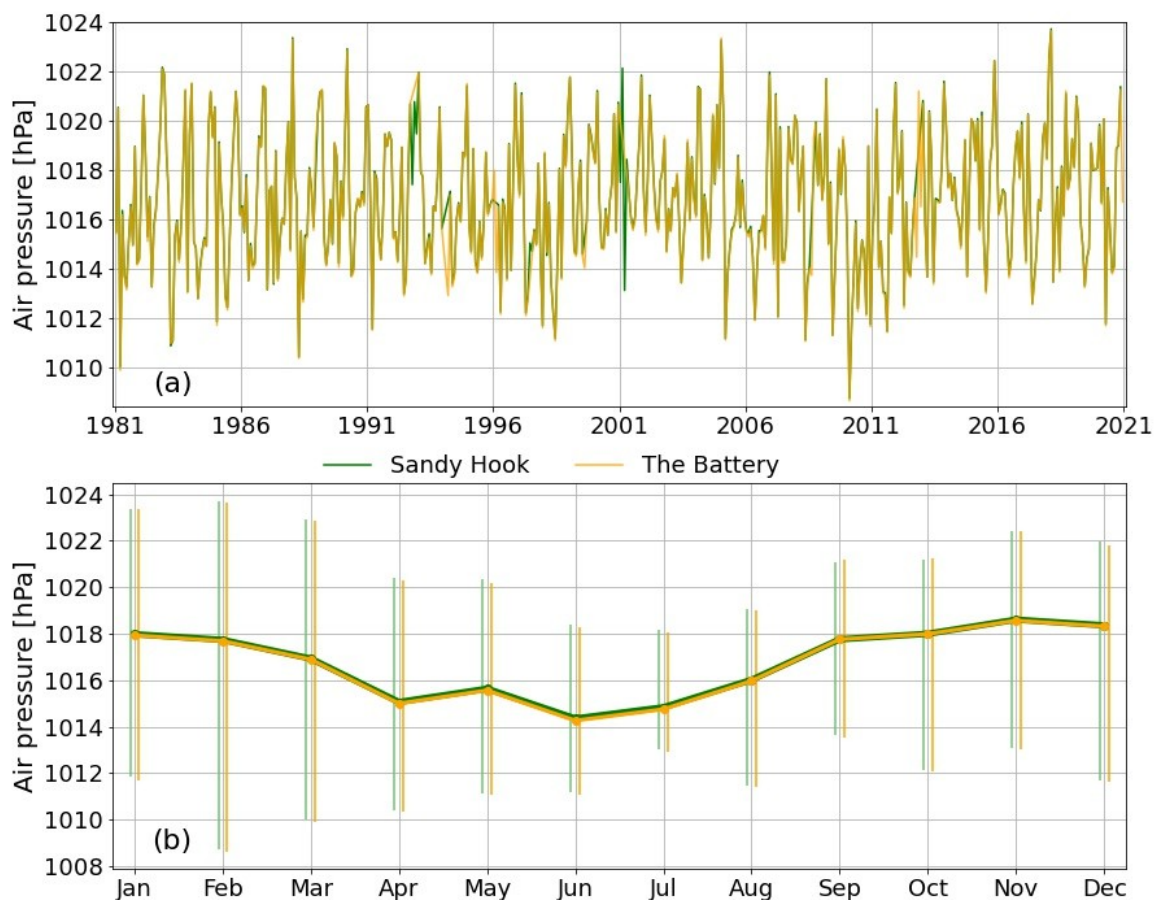
**Figure 13:** Monthly mean from 1981 to 2020 and annual cycle of air pressure on mean sea level or two separate ERA5 data points closest to the sea-level stations at Sandy Hook and The Battery – In **(a)**, the monthly data is displayed. **(b)** shows the mean air pressure for each month of the year as an average of the respective months from 1981 to 2020. The vertical lines represent the range from the maximum to minimum values.

was on February 13, 1981 with over 1051 hPa and the lowest on March 14, 1993 with less than 962 hPa. The latter corresponds to the '1993 Storm of the Century', an enormous blizzard which stretched more than 3500 km from Canada to Honduras. There are slightly larger deviations between the data points in 1992 and in the winter of 2000/2001, which is somewhat surprising due to the geographical proximity. That may be caused by the land-sea difference. For the long term, no trend can be discerned for either location. Within the mean seasonal cycle (Fig. 13b), the air pressure hardly changes. In the winter half-year the pressure is slightly higher than during summer. Possibly, this is because the extremely low pressures of the hurricanes in summer outweigh the winter cyclones. Accordingly, the half-year dominance of the air pressure directly opposes the dominance relations regarding the winds.

3.1.4 River Discharge

After multiplying the river discharge of the Hudson River in Green Island, NY by a factor of 1.6, values were obtained that can be used for 'The Battery'. There is little point to link this data with 'Sandy Hook' as this station is not located on the river mouth but at the other end of the bay, where smaller rivers such as the Raritan River also drain. Therefore another correction factor would be needed, which is not provided anywhere in literature. Nonetheless, the Hudson River estuary can be expected to be the dominant component in the local runoff system. In addition to the pressure values, the '1993 Storm of the Century' can also be detected in the river discharge data (Figure 14). The maximum value of roughly 2800 m³/s is in April 1993,
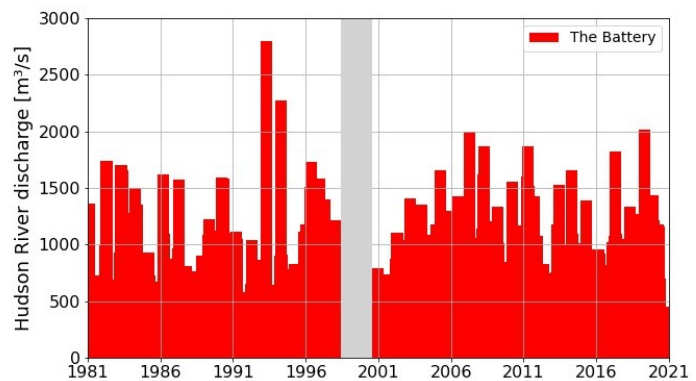

Figure 14: Monthly mean river discharge of the Hudson River. The data from Green Island, NY was multiplied by the factor 1.6 to receive values for 'The Battery'. The grey bar indicates the period in which no data is available.

shortly after the storm. Another maximum is in April 1994, although no blizzard, hurricane or other strong storm event occurred beforehand. The increased river discharge may be explained by high precipitation or late sudden snow melt. All other higher deflections from the mean of $429.8\,\mathrm{m^3/s}$ can usually be found in spring or after storms and are likely to relate to the preceding factors. As with wind energy and pressure, no clear long-term trend for the discharge is evident.

3.2 Correlations with the Sea Level

First, the correlations between sea level and sectorial wind energy are considered. They are shown graphically in Figure 15. The distribution in the same
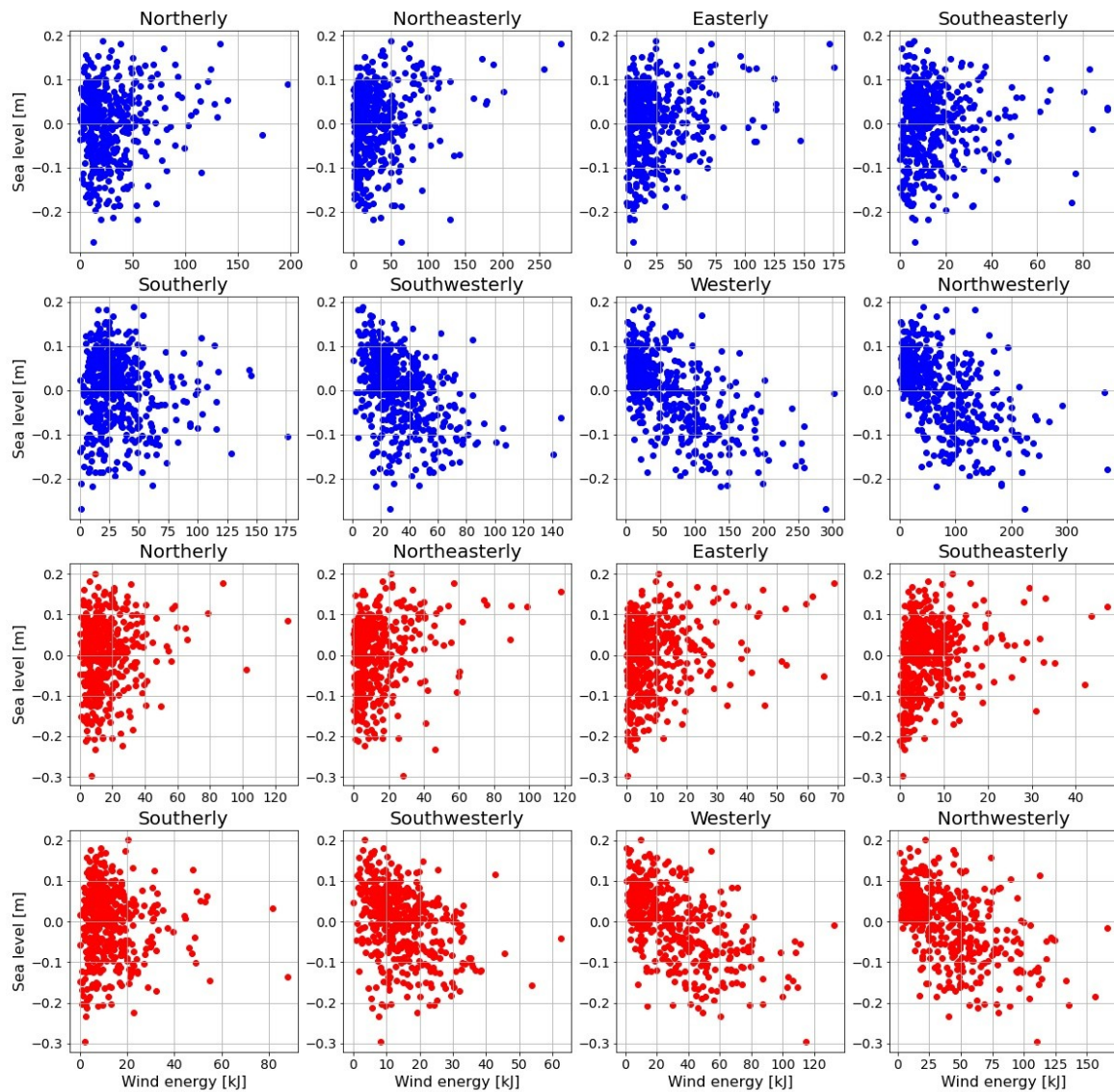
Figure 15: Scatter plots for the correlations between the individual wind energy sectors and the sea level - The top eight plots (blue) depict the properties for 'Sandy Hook' and the associated data point from the ERA5 reanalysis. The bottom eight for 'The Battery'.

sectors looks similar for both sea level stations. In some sectors, e.g. the southerly, there are almost completely unsorted point clouds. For others, however, especially those with a westerly component, a linear dependency can be derived, so that the assumption made at the beginning seems to be adequate. The northerly and southerly wind sector appears to be particularly uncorrelated to the sea level. In these cases the wind blows fairly parallel to the coast.

VARIABLE	SANDY HOOK		THE BATTERY	
	COEFFICIENT	SIGNIFICANCE	COEFFICIENT	SIGNIFICANCE
Northerly wind energy E_N	0.072	< 95%	0.120	< 95%
Northeasterly E_{NE}	0.235	99%	0.223	99%
Easterly E_E	0.198	99%	0.192	99%
Southeasterly E_{SE}	0.064	< 95%	0.206	99%
Southerly E_S	-0.085	< 95%	-0.049	< 95%
Southwesterly E_{SW}	-0.428	99%	-0.369	99%
Westerly E_W	-0.604	99%	-0.577	99%
Northwesterly E_{NW}	-0.548	99%	-0.532	99%
Air pressure p	-0.376	99%	-0.352	99%
Hudson River discharge Q	–	–	-0.127	< 95%

Table 2: Coefficients for Pearson correlation of ERA5-reanalysis values and Hudson River discharge with the sea level

The graphical analysis is confirmed by the correlation coefficients (Table 2). At both SH and TB, there is no significant correlation (< 95%) between northerly or southerly wind energy and sea level. Additionally, the southeasterly wind energy does not provide statistical significance for SH (< 95%). In contrast, all other sectors are even highly significant (99%) and will still be further observed. When considering the remaining parameters, air pressure is also highly significant (99%). However, the river discharge is not significant, although only by a narrow margin (~95%) and will therefore still be taken into account. Negative correlation coefficients are found for air pressure, river discharge and for all wind energy sectors with a westerly component. Analogously, all sectors with an easterly component are associated with a positive coefficient. In this context, a negative coefficient implies a decrease in sea level due to the increase of the corresponding

parameter. Looking at the bay's geography, the negative correlations for the winds can easily be explained by the fact that winds with a westerly component push the water out of the bay and accordingly lower the sea level. Also, increased air pressure, and surprisingly river discharge, lower the sea level. On the one hand, it is conceivable that increased runoff also means increased water volume in the bay and accordingly increased sea level. On the other hand, increased discharge may prevent water from the Atlantic from flowing into the bay, and thus lowering the sea level. Because of the correlation coefficient, the latter seems to be the case. But either way, the discharge is to be viewed with caution due to the correlation being close to the threshold value for the statistical significance of ±0.128.

Overall, according to the coefficients, wind energy from the west (-0.604/ -0.577), northwest (-0.548/ -0.532) and southwest (-0.428/ -0.369) have the greatest impacts on sea level. The occurrence of the wind sectors within the ERA5 data coincides with the strength of correlation, i.e. these sectors are also represented the most in exactly that order. Though, the value of the coefficient cannot simply be explained by the amount of data points. That is because, in terms of frequency, the sectors with a westerly component are immediately followed by the northerly and southerly sector, which are both not significantly correlated at all.

3.3 Sea Level Reconstruction

With help of a multivariate regression, it was possible to reconstruct the sea level for both stations with the inspected parameters that offer a significant correlation. The method is explained in Section 2.4 and the respective coefficients are displayed in Table 3. For 'Sandy Hook', the air pressure and all wind energy sectors except for the northerly, southeasterly and southerly were used (Fig. 16a). The same applies to 'The Battery', whereby the southeasterly wind energy was taken into account as well and used both with (Fig. 16c) and without the Hudson River discharge (Fig. 16b).

Variable	Unit of the Coefficient	Sandy Hook Coefficient	The Battery Coefficient with Q	The Battery without Q
Intercept b	[m]	9096.757	9279.248	9560.587
Northerly E_N	[m/J]	–	–	–
Northeasterly E_{NE}	[m/J]	$4.732 \cdot 10^{-4}$	$9.053 \cdot 10^{-4}$	$9.359 \cdot 10^{-4}$
Easterly E_E	[m/J]	$3.864 \cdot 10^{-4}$	$7.119 \cdot 10^{-4}$	$7.511 \cdot 10^{-4}$
Southeasterly E_{SE}	[m/J]	–	$1.708 \cdot 10^{-3}$	$1.567 \cdot 10^{-3}$
Southerly E_S	[m/J]	–	–	–
Southwesterly E_{SW}	[m/J]	$-7.942 \cdot 10^{-4}$	$-1.403 \cdot 10^{-3}$	$-1.467 \cdot 10^{-3}$
Westerly E_W	[m/J]	$-5.382 \cdot 10^{-4}$	$-1.241 \cdot 10^{-3}$	$-1.264 \cdot 10^{-3}$
Northwesterly E_{NW}	[m/J]	$-3.902 \cdot 10^{-4}$	$-1.004 \cdot 10^{-3}$	$-9.870 \cdot 10^{-4}$
Air pressure p	[m/hPa]	$-8.883 \cdot 10^{-2}$	$-9.065 \cdot 10^{-2}$	$-9.338 \cdot 10^{-2}$
River discharge Q	[s/m^2]	–	$-5.758 \cdot 10^{-3}$	–

Table 3: Coefficients of a multivariate regression for a reconstruction of the sea level at 'Sandy Hook' and 'The Battery'. Based on ERA5-reanalysis and Hudson River discharge data Q from Green Island, NY. Because of the insufficient significance of Q, the calculation for TB was executed both with and without Q. All other variables for which no coefficient was given have too low significance.
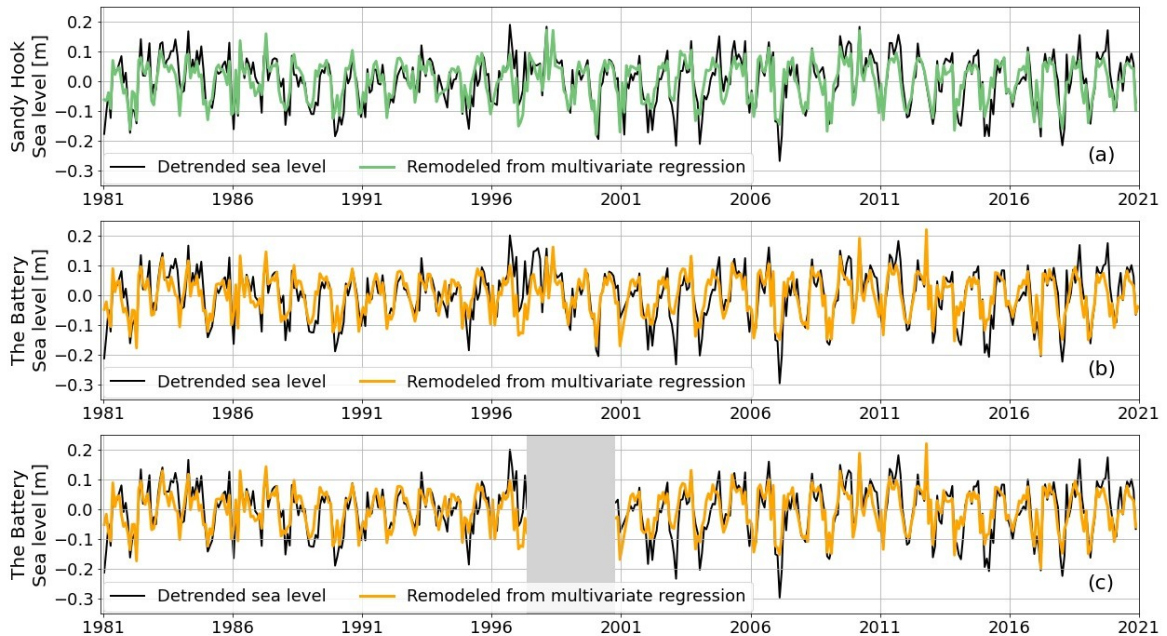
Figure 16: Reconstructed sea levels for both sea level stations – The black lines indicate the monthly mean detrended values of the actual measured sea level. The coloured lines (green and orange) represent calculated monthly values through a multivariate regression with atmospheric data from the ERA5-reanalysis for 'Sandy Hook' **(a)** and 'The Battery' **(b)**. Another multivariate regression was done for 'The Battery' with an additional use of the Hudson River discharge data **(c)**. The grey bar indicates the period in which no discharge data is available.

At first glance, the curves of all reconstructed sea levels (RSL) correspond closely to the observed monthly values of the detrended sea level. Positive and negative deflections are generally well met by the RSL. However, the RSL does not agree well with particularly large deviations of the sea level from the 0 m baseline, such as in 1997, in the early 2000s or 2018 and 2019. When looking specifically at 'The Battery', there is no noticeable difference between the RSL calculated with and without the Hudson River discharge. In fact, the correlation coefficients between the actual detrended sea level at TB and the RSL show an even lower value for the calculation with the discharge (0.785) than without it (0.791). The coefficient for SH is 0.807. Thus, a good remodel can already be executed with the parameters used here. Nevertheless, there are still inaccuracies in the details and the sea level signal is not fully captured. That suggests that there are additional parameters which influence the sea level in the NYB. If the energies of the wind sectors which have too little significance are also considered, the correlation coefficients for the RSL are actually slightly larger (2-3%) but still not close to 1. Subtracting the RSL from the detrended measured values results in the remaining signal of additional parameters that potentially influence the sea level (Figure 17). In general, the fluctuations are no longer as strong as with the actual course of the sea level. Still, individual events can be recognised, by means of which one could identify the remaining parameters. These include deflections of the remaining signal of up to 0.2 m, which is more than the actual fluctuation of the sea level most of the time. For over 70% of the period though, the difference does not exceed ±0.05 m.
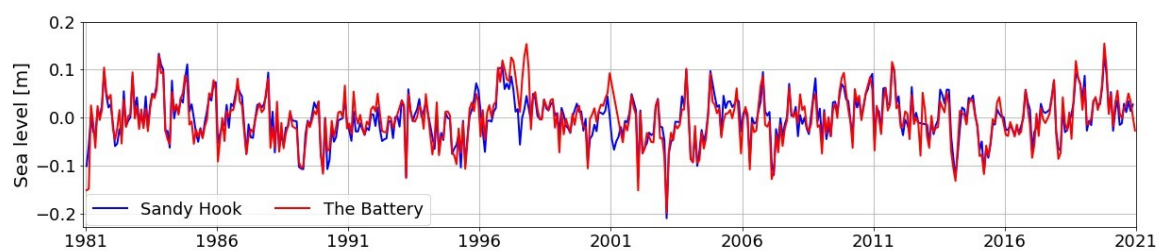
Figure 17: Remaining signal after removing the reconstructed sea level of the ERA5-reanalysis from the actual measured detrended sea level values

4 Discussion

In the previous sections, numerous calculations were carried out and the parameters were viewed from different perspectives. All of this served to answer the questions posed in the introduction, which will be taken up in the following sections. First, in order to work with the results and to verify the interpretations, it helps to keep the quality of the datasets and calculations in mind.

4.1 Limitations of the Datasets

For a proper analysis, it is of course necessary to have reasonable datasets. In retrospect, however, this was not fundamentally the case. Long time periods are available for sea level data, but only on a monthly basis and occasionally even with missing values. As a result, it was impossible to record all fluctuations in the fast-moving wind. Only large storm events were detectable, which still was sufficient for an assessment of the influential parameters. In terms of spatial resolution, both main regions of New York Bay were covered by the sea level stations – one almost on the open sea ('Sandy Hook') and one at the Hudson River mouth in the innermost corner of the bay ('The Battery').

Atmospheric measurement data is not available for long periods for the inspected area. Thus, it was reasonable to use a reanalysis as they usually cover large time spans. The ERA reanalyses, for example, are getting more precise and are even partially based on measurement records (Hersbach et al., 2020). An advantage of this is that there are no data gaps like there are with the sea level data. Unfortunately though, not every value is 100% realistic and reliable. Furthermore, the here used ERA5 provides a weak resolution which makes it hard to assess regional variability. The grid is useful for a global analysis but for New York Bay, only two data points were suitable. At least they were conveniently located at the sea level stations and actually offered reasonable values that

differed from one another. A next step would be to validate the ERA5 data in available time segments with measurement data for the New York Bay.

Additionally, no discharge data of the Hudson River estuary was available for New York City. It is questionable whether only a correction by a factor of 1.6 for the Green Island data is sufficient. Ralston et al. (2008), who state to have achieved good results with the data, used it in comparison with a model. However, only the general course of their model and the corrected Green Island data was the same but not individual deflections, especially not during high river discharge events. Though, since only monthly averages were taken from the daily data, this is probably not of great relevance. Furthermore, the lower part of the Hudson River from the data station in Green Island to 'The Battery' is a fairly straight stream and does not consist of complex drainage and flow patterns such as the upper part (Levinton and Waldman, 2006). Therefore, the approximation may be justified.

Due to the aspects mentioned above, the datasets were adequate in terms of quality but the results could certainly be augmented if there was better spatial and temporal record coverage available.

4.2 Differences of 'Sandy Hook' and 'The Battery' to the Global Trend

At the beginning of the data analysis, it struck first that the regional sea level rise is greater than in the global mean. Horton et al. (2015) state that New York City is particularly affected by land subsidence due to glacial isostatic adjustment in the long-term trend. According to Kemp and Horton (2013), this aspect accounts for at least 25% of the local increase, and it is a general phenomenon which can be observed along the North American Atlantic coast (Sallenger et al., 2012). Furthermore, the long-term trend at 'Sandy Hook' is even stronger than at 'The Battery', although both stations are close to each other. This can be explained by the higher exposure of SH to the sea. Hence, even within a small bay, there are differences in the local properties.

4.3 Wind as the Dominant Parameter on Interannual Timescales

The results show that the wind, especially with a westerly component, is a dominant driver. Also Choi and Wilkin (2007) argue that westerly winds increase water transport out of the bay, thereby lowering sea levels. Consequently, the non-existent correlation for northerly and southerly wind energy with sea level can be derived. Since in those cases, the winds blow parallel to the coast and the New York Bay's entrance, water is neither pushed in nor out of the bay. Nevertheless, winds of these two directions have an indirect influence on the bay by accelerating or decelerating the flow velocity of the Hudson River, which runs in north-south direction (Ralston et al., 2008). The remaining correlation coefficients are highly significant but with a maximum value of -0.604 they are not particularly large. Elsewhere, e.g., in the Dutch Wadden Sea, the coefficients can be up to ±0.8 for the westerly and easterly components (Gerkema and Duran-Matute, 2017). However, at that location, wind speeds since 2000 are on average twice as high as at SH (Windfinder, 2021). Accordingly, the wind energies are even eight times higher, which explains why the wind is even more influential there.

Since the main wind direction is west-northwesterly, some wind peaks seem to get divided between these two sectors. Therefore, it should be considered to subdivide the wind energies not into 8 sectors but only into a west-east component or to even further split them into 16 sectors.

In the future it is to be expected that the hydrodynamics of the bay will further change. This can be due to the fact that fairways are dredged (Ralston et al., 2018) or the storm protection walls mentioned at the beginning are built. Extreme wind events also cause sediment transport which influences the hydrodynamics (Ralston et al., 2013). As a result, the distribution of the dominant wind energy sectors could also change.

4.4 Further Influential Parameters

In addition to wind, the air pressure on mean sea level showed a comparatively high correlation coefficient. Pressure is also mentioned as a highly influential parameter for the New York City area by Colle et al. (2010) and Orton et al. (2012). The latter and Piecuch et al. (2018) state that freshwater fluxes have a major impact on the local sea level as well, especially during large storm events such as the 'Nor'easters'. However, this could not be confirmed by this thesis. This may be due to the inaccuracies and disadvantages of the available discharge data, as explained in Section 4.1. Furthermore, there are smaller rivers such as the Raritan River (as inspected in Choi and Wilkin, 2007), or the Newark Bay estuary which drain into Raritan Bay. Raritan Bay is directly west of Lower New York Bay, and is likely to have an influence as a connected water body. Precipitation also belongs to the freshwater fluxes and could therefore be treated as an individual variable, but it is already indirectly included in the Hudson River discharge data. Other parameters on daily or hourly time scales are the lunar cycle and tides. The amplitude between low tide and high tide is influenced by the lunar cycle, but this is neither captured nor essential in mean values, let alone in monthly means (Gerkema and Duran-Matute, 2017). Since thermal expansion effects dominate the long-term trend, incoming solar radiation or sea surface temperature could also be taken into account.

4.5 Conclusion and Outlook

All in all, sea levels in the New York Bay have risen steadily in the period from 1981 to 2020. Winds with a westerly component showed the largest influence in this thesis but air pressure and winds with an easterly component also account for variations in sea level. Hudson River discharge, wind and air pressure data did not seem to present any long-term trend. A multiple regression was used to reconstruct the sea levels at the stations 'Sandy Hook' and 'The Battery' with the

respective correlation coefficients. Although the reconstruction in this thesis does not entirely agree with the actual measurement data, it offers a good approach. Yet, additional parameters such as further discharge data, precipitation or solar radiation could be taken into account since the sea level is left with a certain signal after a detrend and correction for the wind and air pressure. That could be supplemented by validating the ERA5 reanalysis in the New York Bay with small available sections of measurement data. Together with the parameters already used, a new reconstruction of the sea level would be interesting which could then be used together with climate models to project future local sea level variations. However, the changing hydrodynamics of New York Bay must also be considered.

As an alternative, the whole procedure could be reversed by first determining the interannual variabilities in order to then obtain a corrected long-term trend. That would follow a completely different approach and could result in useful additions to the subject.

References

ADD-RLP (Aufsichts- und Dienstleistungsdirektion Rheinland-Pfalz) (2021): Zahlen und Fakten. *Aktuelle Lage im Hochwassergebiet Ahrweiler*. Retrieved November 3, 2021, from https://hochwasser-ahr.rlp.de/de/aktuelle-lage/zahlen-und-fakten/

Aon (2021): Global Catastrophe Recap July 2021. *Reinsurance Thought Leadership*. Retrieved November 8, 2021, from http://thoughtleadership.aon.com/Documents/20211008_analytics-if-july-global-recap.pdf

ASCE (American Society of Civil Engineers) (1994): Seven Wonders. Retrieved November 10, 2021, from https://web.archive.org/web/20121026093022/http://www.asce.org/People-and-Projects/Projects/Seven-Wonders/Seven-Wonders/

Blake, E.S., Kimberlain, T.B., Berg, R.J., Cangialosi, J.P., & Beven, J.L. (2013): AL182012 Hurricane Sandy, Tropical Cyclone Report. *National Hurricane Center*, *157*.

BMI (Bundesministerium des Innern, für Bau und Heimat) (2021): Zwischenbericht zur Flutkatastrophe – Katastrophenhilfe, Soforthilfen und Wiederaufbau. Retrieved November 14, 2021 from https://www.bundesregierung.de/resource/blob/974430/1963706/613b934d3f359a5118df16755e9e527c2021-09-27-zwischen bericht-hochwasser-data.pdf?download=1

Bowman, M.J., & Flood, R.J. (2002): Hydrologic feasibility of storm surge barriers to protect the metropolitan New York – New Jersey region.

Brito, P., Lopes, P., Reis, P., & Alves, O. (2014): Simulation and optimization of energy consumption in cold storage chambers from the horticultural industry. *International Journal of Energy and Environmental Engineering*, *5*(2–3).

Bull, G.A. (1952): Smithsonian Meteorological Tables. *Nature*, *170*(4318), 175.

CEG (Construction Equipment Guide Newspapers) (2021): NYC's Living Breakwaters Project Builds Barriers to Fight Rising Seas. *Northeast Edtion*. Retrieved December 5, 2021, from https://www.constructionequipmentguide.com/nycs-107m-living-breakwaters-project-building-barriers-to-fight-rising-seas/54449

Choi, B.J., & Wilkin, J.L. (2007): The Effect of Wind on the Dispersal of the Hudson River Plume. *Journal of Physical Oceanography, 37*(7), 1878–1897.

Colle, B.A., Buonaiuto, F., Bowman, M.J., Wilson, R.E., Flood, R., Hunter, R., Mintz, A., & Hill, D. (2008): New York City's Vulnerability to Coastal Flooding. *Bulletin of the American Meteorological Society*, *89*(6), 829–842.

Colle, B.A., Rojowsky, K., & Buonaito, F. (2010): New York City Storm Surges: Climatology and an Analysis of the Wind and Cyclone Evolution. *Journal of Applied Meteorology and Climatology*, *49*(1), 85–100.

Firtina-Ertis, I., Acar, C., & Erturk, E. (2020): Optimal sizing design of an isolated stand-alone hybrid wind-hydrogen system for a zero-energy house. *Applied Energy*, *274*, 115244.

Gerkema, T., & Duran-Matute, M. (2017): Interannual variability of mean sea level and its sensitivity to wind climate in an inter-tidal basin. *Earth System Dynamics*, *8*(4), 1223–1235.

Guan, C., & Xie, L. (2004): On the Linear Parameterization of Drag Coefficient over Sea Surface. *Journal of Physical Oceanography*, *34*(12), 2847–2851.

Hersbach, H., Bell, B., Berrisford, P., Hirahara, S., Horányi, A., Muñoz-Sabater, J., Nicolas, J., Peubey, C., Radu, R., Schepers, D., Simmons, A., Soci, C., Abdalla, S., . . . Thépaut, J. (2020): The ERA5 global reanalysis. *Quarterly Journal of the Royal Meteorological Society*, *146*(730), 1999–2049.

Hill, D. (2008): Must New York City Have Its Own Katrina? *Leadership and Management in Engineering*, *8*(3), 132–138.

Holgate, S.J., Matthews, A., Woodworth, P.L., Rickards, L.J., Tamisiea, M.E., Bradshaw, E., Foden, P.R., Gordon, K.M., Jevrejeva, S., & Pugh, J. (2013): New Data Systems and Products at the Permanent Service for Mean Sea Level. *Journal of Coastal Research, 29*(3), 493-504.

Horton, R., Little, C., Gornitz, V., Bader, D., & Oppenheimer, M. (2015): New York City Panel on Climate Change 2015 Report Chapter 2: Sea Level Rise and Coastal Storms. *Annals of the New York Academy of Sciences*, *1336*(1), 36–44.

IPCC (Intergovernmental Panel on Climate Change) (2021): Summary for Policymakers. In: Climate Change 2021: The Physical Science Basis. Contribution of Working Group I to the Sixth Assessment Report of the Intergovernmental Panel on Climate Change [Masson-Delmotte, V., Zhai, P., Pirani, A., Connors, S.L., Péan, C., Berger, S., Caud, N., Chen, Y., Goldfarb, L., Gomis, M.I., Huang, M., Leitzell, K., Lonnoy, E., Matthews, J.B.R., Maycock, T.K., Waterfield, T., Yelekçi, O., Yu, R., and Zhou, B. (eds.)]. Cambridge University Press. In Press.

Kemp, A.C., & Horton, B.P. (2013): Contribution of relative sea-level rise to historical hurricane flooding in New York City. *Journal of Quaternary Science*, *28*(6), 537–541.

KSU (Kent State University) (2021): Pearson Correlation. *LibGuides: SPSS Tutorials*. Retrieved December 1, 2021, from https://libguides.library.kent.edu/SPSS/PearsonCorr

Lerczak, J.A., Geyer, W.R., & Chant, R.J. (2006): Mechanisms driving the time-dependent salt flux in a partially stratified estuary. *Journal of Physical Oceanography*, 36, 2283-2298.

Levinton, J.S., & Waldman, J.R. (Eds.) (2006): The Hudson River Estuary. Cambridge University Press Cambridge, UK.

NASA (National Aeronautics and Space Administration) (2021): Sea Level Satellite Data: 1993 - present. *Global Climate Change – Vital Signs of the Planet*. Retrieved November 2, 2021, from https://climate.nasa.gov/vital-signs/sea-level/

National Hurricane Center (2021a): Tropical Cyclone Climatology. National Oceanic and Atmospheric Administration (NOAA). Retrieved November 7, 2021, from https://www.nhc.noaa.gov/climo/

National Hurricane Center (2021b): Glossary of NHC Terms. National Oceanic and Atmospheric Administration (NOAA). Retrieved December 6, 2021, from https://www.nhc.noaa.gov/aboutgloss.shtml#SEASON

National Weather Service (2016): Hurricane Katrina August 2005. National Oceanic and Atmospheric Administration (NOAA). Retrieved October 31, 2021, from https://www.weather.gov/mob/katrina

Orton, P., Georgas, N., Blumberg, A., & Pullen, J. (2012): Detailed modeling of recent severe storm tides in estuaries of the New York City region. *Journal of Geophysical Research: Oceans*, *117*(C9).

Piecuch, C.G., Bittermann, K., Kemp, A.C., Ponte, R.M., Little, C.M., Engelhart, S.E., & Lentz, S.J. (2018): River-discharge effects on United States Atlantic and Gulf coast sea-level changes. *Proceedings of the National Academy of Sciences*, *115*(30), 7729–7734.

PSMSL (Permanent Service for Mean Sea Level) (2021a): Sandy Hook – RLR Information. Retrieved November 17, 2021, from https://www.psmsl.org/data/obtaining/rlr.diagrams/366.php

PSMSL (Permanent Service for Mean Sea Level) (2021b): The Battery – RLR Information. Retrieved November 17, 2021, from https://www.psmsl.org/data/obtaining/rlr.diagrams/12.php

Ralston, D.K., Geyer, W.R., & Lerczak, J.A. (2008): Subtidal Salinity and Velocity in the Hudson River Estuary: Observations and Modelling. *Journal of Physical Oceanography*, *38*(4), 753–770.

Ralston, D.K., Warner, J.C., Geyer, W.R., & Wall, G.R. (2013): Sediment transport due to extreme events: The Hudson River estuary after tropical storms Irene and Lee. *Geophysical Research Letters*, *40*(20), 5451–5455.

Ralston, D.K., Talke, S., Geyer, W.R., Al-Zubaidi, H.A.M., & Sommerfield, C.K. (2019): Bigger Tides, Less Flooding: Effects of Dredging on Barotropic Dynamics in a Highly Modified Estuary. *Journal of Geophysical Research: Oceans, 124*(1), 196–211.

Royte, E. (2019): Could Massive Storm Surge Barriers End the Hudson River's Revival? *YaleEnvironment360*. Retrieved November 3, 2021, from https://e360 .yale.edu/features/could-massive-storm-surge-barriers-end-the-hudson-rivers-revival

Sallenger, A., Doran, K. & Howd, P. (2012): Hotspot of accelerated sea-level rise on the Atlantic coast of North America. *Nature Clim Change* 2, 884–888.

Schlatter, T.W., & Baker, D.V. (1991): Algorithms, Comparisons and Source References by Schlatter and Baker. *Shelquist Engineering*. Retrieved October 19, 2021, from https://wahiduddin.net/calc/density_algorithms.htm

Stephenson, D.B., & Kolli, R.K. (1997): Correlation Coefficient – Critical values for Testing Significance. Retrieved December 1, 2021, from https://empslocal.ex .ac.uk/people/staff/dbs202/cat/stats/corr.html

Tijburg, P. (2021): How Much Of The Netherlands Is Below Sea Level? *Netherlands Insiders*. Retrieved December 3, 2021, from https://netherlandsinsiders.com/ how-much-of-the-netherlands-is-below-sea-level/

U. S. Census Bureau (2019): Population Estimates - NJ: Bergen County, Union County, Hudson County, Middlesex County, Monmouth County; NY: New York City. Retrieved November 9, 2021, from https://www.census.gov/quickfacts/ fact/table/bergencountynewjersey,unioncountynewjersey,hudsoncountynewje rsey,newyorkcitynewyork,middlesexcountynewjersey,monmouthcountynewje rsey/PST045219

Windfinder (2021): Wind and weather statistic Vlieland Vliehors. Retrieved October 21, 2021, from https://www.windfinder.com/windstatistics/vlieland

World Ocean Review 1 (2010): Living with the oceans – A report on the state of the world's oceans. *Future of Ocean Kiel, International Ocean Institute Malta, and maribus gGmbH.*

Zhong, H., van Overloop, P.-J., & van Gelder, P.H.A.J.M. (2013): A joint probability approach using a 1-D hydrodynamic model for estimating high water level frequencies in the Lower Rhine Delta, *Nat. Hazards Earth Syst. Sci.*, 13, 1841 1852.

Acknowledgements

Eidesstattliche Erklärung

Hiermit versichere ich, Leon-Cornelius Mock, dass ich die Bachelorarbeit

'Sea Level Variations in the New York Bay due to Various Parameters'

eigenständig und ohne Benutzung anderer als der angegebenen Quellen und Hilfsmittel verfasst habe und zudem alle inhaltlichen und wörtlichen Zitate als solche gekennzeichnet habe. Diese Arbeit hat in gleicher oder ähnlicher Form noch keiner Prüfungsbehörde vorgelegen. Zudem versichere ich, dass die von mir abgegebenen schriftlichen gebundenen Versionen der vorliegenden Arbeit mit der elektronischen Version auf einer CD-ROM inhaltlich übereinstimmen.

Statutory Declaration

I, Leon-Cornelius Mock, herewith confirm that I have written the bachelor thesis

'Sea Level Variations in the New York Bay due to Various Parameters'

independently and without the use of any other than the cited sources and aids. I have also marked all literal and content citations as such. This thesis has not been submitted to any examination body in the same or a similar form before. Furthermore, I declare that the submitted written copies of the present thesis and the version on a CD-ROM are consistent with each other in contents.

Place, Date: ....   **Signature:** ....